

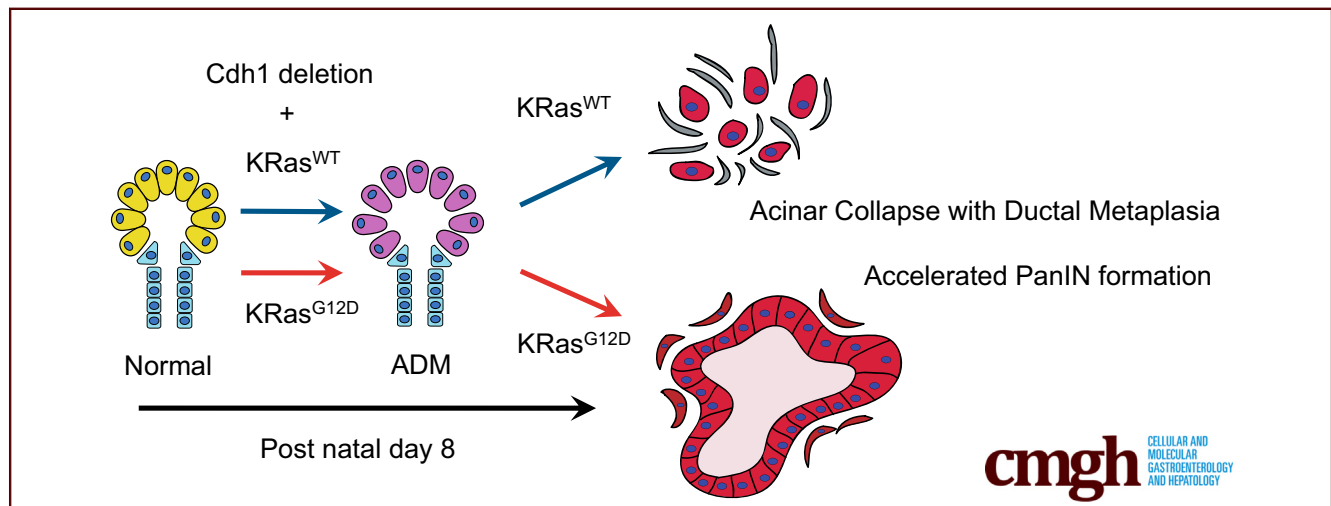
ORIGINAL RESEARCH

Loss of Pancreatic E-Cadherin Causes Pancreatitis-Like Changes and Contributes to Carcinogenesis



Yoshihiro Kaneta,¹ Takeshi Sato,¹ Yohko Hikiba,¹ Makoto Sugimori,¹ Soichiro Sue,¹ Hiroaki Kaneko,¹ Kuniyasu Irie,¹ Tomohiko Sasaki,¹ Masaaki Kondo,¹ Makoto Chuma,² Wataru Shibata,^{1,3} and Shin Maeda¹

¹Department of Gastroenterology, Graduate School of Medicine, ²Advanced Medical Research Center, Yokohama City University, Yokohama, Japan; ³Gastroenterological Centre, Yokohama City University Medical Centre, Yokohama, Japan



SUMMARY

We created a mouse model in which E-cadherin in the pancreas was specifically deleted. Loss of E-cadherin resulted in pancreatitis-like changes under physiological conditions and contributed to carcinogenesis in the presence of an oncogene.

BACKGROUND & AIMS: E-cadherin (*Cdh1*) is a key molecule for adherence required for maintenance of structural homeostasis. Loss of E-cadherin leads to poor prognosis and the development of resistance to chemotherapy in pancreatic cancer. Here, we evaluated the physiological and pathologic roles of E-cadherin in the pancreas.

METHODS: We crossbred *Ptf1a-Cre* mice with *Cdh1^{fl/fl}* mice to examine the physiological roles of E-cadherin in the pancreas. In addition, we crossbred these mice with *LSL-Kras^{G12D/+}* mice (PKC) to investigate the pathologic roles of E-cadherin. We also generated a tamoxifen-inducible system (*Ptf1a-Cre^{ERT}* model). Organoids derived from these models using lentiviral transduction were analyzed for immunohistochemical features. Established cell lines from these organoids were analyzed for migratory and invasive activities as well as gene expression by complementary DNA microarray analyses.

RESULTS: None of the *Ptf1a-Cre* mice crossbred with *Cdh1^{fl/fl}* mice survived for more than 28 days. We observed aberrant epithelial tubules that resembled the structure of acinar-ductal metaplasia after postnatal day 6, showing features of pancreatitis. All of the PKC mice died within 10 days. We observed tumorigenicity with increasing stroma-like aggressive tumors. *Ptf1a-Cre^{ERT}* models showed that deletion of E-cadherin led to earlier pancreatic intraepithelial neoplasm formation. Cells established from PKC organoids had greater migratory and invasive activities, and these allograft tumors showed a poorly differentiated phenotype. Gene expression analysis indicated that *Hdac1* was up-regulated in PKC cell lines and a histone deacetylase 1 inhibitor suppressed PKC cell proliferation.

CONCLUSIONS: Under physiological conditions, E-cadherin is important for maintaining the tissue homeostasis of the pancreas. Under pathologic conditions with mutational *Kras* activation, E-cadherin plays an important role in tumor formation via the acquisition of tumorigenic activity. (*Cell Mol Gastroenterol Hepatol* 2020;9:105–119; <https://doi.org/10.1016/j.jcmgh.2019.09.001>)

Keywords: Pancreas; Oncogene; Gene Regulation; Pancreatic Cancer; E-Cadherin.

See editorial on page 191.

E-cadherin is a Ca^{2+} -dependent adhesion protein belonging to the classic cadherin family. Physiologically, the classic cadherins play important roles in cell-to-cell adhesion and epithelial polarity. Although E-cadherin is one of the constituent members of adherens junctions, it also is responsible for intracellular signaling and gene transcription.^{1,2}

E-cadherin knockout mice die at an early embryonic stage and, therefore, conditional knockout mice have been used in studies. For example, deletion of E-cadherin in skin impaired epidermal barrier function, resulting in death at the neonatal stage.³ We reported previously that deletion of E-cadherin in the liver leads to the development of periportal inflammation resembling sclerosing cholangitis via impairment of the intrahepatic biliary network.⁴ Therefore, E-cadherin plays an important role in tissue homeostasis, although its roles differ among organs.

With regard to the pancreas, previous studies have indicated that E-cadherin expression was up-regulated in rodent models of chemically induced acute pancreatitis. This reaction was considered to be a response to protect and repair cell–cell adhesions of pancreatic acinar cells.^{5,6} On the other hand, chronic pancreatitis, which is associated with a high risk of pancreatic adenocarcinoma (PDAC), showed low or no expression of E-cadherin.⁷ However, the precise functional role of E-cadherin in the pancreas still is unknown, especially *in vivo*.

It has been reported that alteration of E-cadherin expression contributes to cancer progression.⁴ In human gastric cancer, loss of E-cadherin has been linked with diffuse-type cancer,⁸ and germline-inactivating mutations in the E-cadherin gene are characteristic of hereditary diffuse gastric cancer syndrome.⁹ Loss of E-cadherin has organ-specific effects (eg, liver, stomach, skin, or mammary gland), such as inflammation, hyperproliferation, and promotion of tumor formation.^{4,10–12} In pathogenic states, E-cadherin has been reported as a marker of morphologic changes, such as epithelial–mesenchymal transition (EMT), but there is little evidence that cancers undergo EMT by deletion of E-cadherin.

Pancreatic cancer is the third leading cause of cancer-related deaths, with a 5-year relative survival rate of 8%. The majority of patients are diagnosed at an advanced stage, for which the 5-year survival rate is 3%.¹³ Reduction of E-cadherin expression in pancreatic cancer is observed especially in undifferentiated cancers and is correlated with EMT induction and poor prognosis.¹⁴ Transcriptional repressors, such as Snail, Slug, and Twist, play important roles in induction of EMT, and E-cadherin is a major target of these factors. However, it is unclear whether the loss of E-cadherin is a real regulator of EMT induction and pancreatic cancer development.¹⁵

Therefore, we investigated the roles of E-cadherin in the pancreas and pancreatic tumor development using pancreas-specific E-cadherin knockout mice.

Results


Cdh1 Is Required for Growth and Maintenance of the Pancreas

To examine the physiological roles of E-cadherin in the pancreas, we crossbred homozygous loxP-flanked alleles of *Cdh1* (*Cdh1^{fl/fl}*) mice with pancreas transcription factor 1a (*Ptf1a*)-Cre transgenic mice expressing Cre recombinase from the *Ptf1a* promoter (*Ptf1a-Cre; Cdh1^{fl/+}*). *Cdh1* heterodeficiency did not contribute to the phenotype. Next, we crossbred *Ptf1a-Cre; Cdh1^{fl/+}* with *Cdh1^{fl/fl}* mice to generate *Ptf1a-Cre; Cdh1^{fl/fl}* mice (named *PC* mice) (Figure 1A). Successful Cre-mediated recombination was assessed by polymerase chain reaction (PCR). *PC* mice were born at the expected Mendelian ratio with a morphologically normal pancreas. During postnatal day 0 (P0) to P2, there were no differences in appearance or histology between *Cdh1^{fl/fl}* and *PC* mice (Figure 1B). However, *PC* mice remained small compared with the controls after P3–P4 (Figure 1C). *PC* mice began to die at P12, and none of the *PC* mice survived for more than 28 days. The pancreatic histology of *PC* mice changed markedly at P6–P15. We observed dilated abnormal acinar cells at P6, and aberrant epithelial tubules structurally resembling acinar-to-ductal metaplasia (ADM) (Figure 1B). There was no E-cadherin expression on the surface of pancreatic acinar cells, whereas E-cadherin-positive cells were observed in ADMs (Figure 1D). These results suggested that E-cadherin was not required for pancreatic development at the embryonic stage but was required for growth and maintenance of the pancreas in the postnatal stage.

Loss of Cdh1 Causes Inflammatory and Fibrotic Changes

We performed immunohistochemistry (IHC) analyses to examine the roles of E-cadherin in the morphologic changes seen in the pancreas of *PC*. *PC* mice had significantly decreased numbers of amylase-positive cells and increased numbers of cytokeratin 19 (CK19)-positive cells, as well as histologic changes reflected by a reduced area of acini and

Abbreviations used in this paper: ADM, acinar-to-ductal metaplasia; α -SMA, α -smooth muscle actin; cDNA, complementary DNA; CK19, cytokeratin 19; DMEM, Dulbecco's modified Eagle medium; EMT, epithelial–mesenchymal transition; γ H2AX, γ histone 2AX; HDAC, histone deacetylase; IHC, immunohistochemistry; Klf, Krüppel-like factor; mRNA, messenger RNA; P, postnatal day; PanIN, pancreatic intraepithelial neoplasm; *PC*, *Ptf1a-Cre; Cdh1^{fl/fl}*; PCR, polymerase chain reaction; PDAC, pancreatic ductal adenocarcinoma; p-ERK, phospho–extracellular signal-regulated kinase; PK, *Ptf1a-Cre; LSL-Kras^{G12D/+}*; PKC, *Ptf1a-Cre; LSL-Kras^{G12D/+}; Cdh1^{fl/fl}*; PKC+C, lenti-*Cdh1* in *Ptf1a-Cre; LSL-Kras^{G12D/+}; Cdh1^{fl/fl}* organoids; PSR, Picro-Sirius red; *Ptf1a*, pancreas transcription factor 1a; RFP, red fluorescent protein; 2D, 2-dimensional; YFP, yellow fluorescent protein.

 Most current article

© 2020 The Authors. Published by Elsevier Inc. on behalf of the AGA Institute. This is an open access article under the CC BY-NC-ND license (<http://creativecommons.org/licenses/by-nc-nd/4.0/>).

2352-345X

<https://doi.org/10.1016/j.jcmgh.2019.09.001>

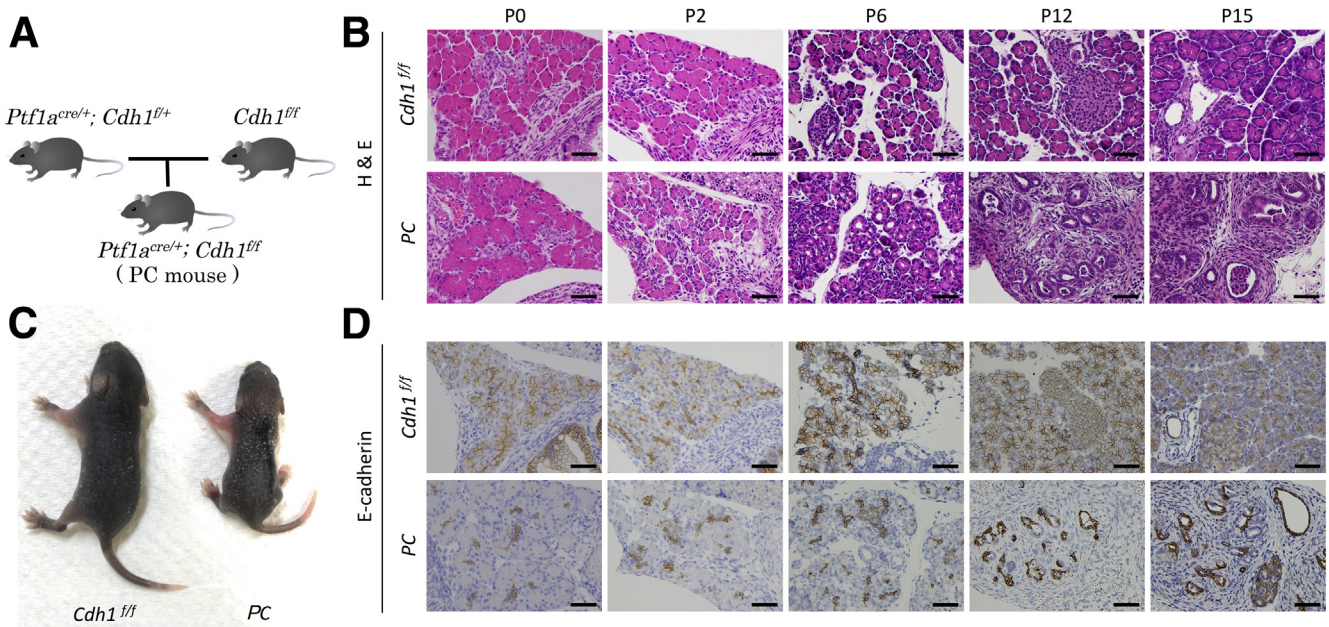


Figure 1. E-cadherin maintains pancreatic homeostasis. (A) Experimental protocol for deleting E-cadherin in the pancreas. (togoTV mouse images was used) (B) H&E staining of the pancreas obtained from $Cdh1^{fl/fl}$ and PC mice on P0–P15. (C) Gross images of $Cdh1^{fl/fl}$ and PC mice on P8. (D) Immunohistochemical analysis of E-cadherin in the pancreas from mice of each genotype and time point. *Upper panels:* Cre-negative mice ($Cdh1^{fl/fl}$). *Lower panels:* Cre-positive mice (PC). Scale bars: 100 μ m.

an increased number of ductal-like structures (Figure 2A and B). The serum amylase level was increased at P6, but decreased at P12, compared with controls, which showed no such changes (Figure 2G). These results also were consistent with the results regarding messenger RNA (mRNA) levels (Figure 2J). At P12–P15, intact areas of acini had almost disappeared, and remaining areas had been replaced by α -smooth muscle actin (α -SMA)-positive fibrotic cells as well as ADMs. Areas with positive Picro-Sirius red (PSR) staining appeared in the stroma, indicating the presence of collagen fibers (Figure 2C and D).

Cells positive for CD45, a marker of leukocyte common antigen, increased over time in the stroma (Figure 2E and H). In addition, relative mRNA expression levels of inflammatory cytokines and chemokines, such as Cxcl2, Ccl2, interleukin 6, and tumor necrosis factor α , were increased at P8 (Figure 2J). Cleaved caspase-3-positive cells, a marker of apoptosis, were nonspecifically observed with $Cdh1^{fl/fl}$ acinar cells, but PC at P6–12 showed strong staining around ductal structures, indicating apoptosis at the sites of ADM formation (Figure 2F). At P15, pancreatic tissue of PC had been almost completely replaced with fibrotic tissue, and cleaved caspase-3 staining in these areas was not clear; all PC mice died by P28 because their pancreas had been functionally compromised by the lack of E-cadherin. These results indicated that loss of E-cadherin in the pancreas caused pancreatitis-like changes accompanied by ADM-like changes. However, we did not observe pancreatic intra-epithelial neoplasia (PanIN), a precursor of PDAC. We quantified the area positive for amylase, cleaved caspase 3, CK19, α -SMA, and PSR in the P6 and P15 pancreas (Figure 2J).

Loss of E-Cadherin Provides Tumorigenic Activity to Pancreatic Cells and Contributes to Carcinogenesis

The mutational activation of *Kras* is the most common genetic mutation in PDAC.¹⁶ To investigate further the pathologic roles of E-cadherin in the pancreas, we cross-bred mice with the *Ptf1a-Cre*, *LSL-Kras^{G12D/+}*, and *Cdh1^{fl/fl}* alleles to generate mice with a combination of oncogenic *Kras^{G12D/+}* expression and *Cdh1* deletion in the pancreas. Previous studies indicated that the *Ptf1a-Cre; LSL-Kras^{G12D/+}* (PK) mouse model started to develop PanIN from 2 weeks of age, and some eventually developed PDAC.^{17,18} We also confirmed that the PK mouse pancreas showed no morphologic changes during P0–P8 (Figure 3A). In contrast, when *Cdh1* deficiency was added to *Kras^{G12D/+}* (*Ptf1a-Cre; LSL-Kras^{G12D/+}; Cdh1^{fl/fl}* [PKC] mice), ADMs and PanINs (low-grade PanIN or PanIN1A/B) were observed at P4–P5, whereas no abnormal changes were observed at P0–P2. The P8 PKC mouse pancreas showed aberrant and dilated ducts corresponding to PanIN-2/3 and desmoplastic reaction-like changes (Figure 3A). PanINs of PKC mice showed partial staining by IHC for E-cadherin at P4–P5, whereas no abnormal changes were observed at P0–P2. The P8 PKC mouse pancreas showed aberrant and dilated ducts corresponding to PanIN-2/3 and desmoplastic reaction-like changes (Figure 3A). PanINs of PKC mice showed partial staining by IHC for E-cadherin at P4–P5. At P7–P8, PanINs of PKC mice also showed partial positive staining for E-cadherin and some showed structural abnormalities, while other lesions in the pancreas showed no staining for E-cadherin (Figure 3B). Decreased amylase staining and increased CK19 staining were observed, as observed in PC mice (Figure 3C and D). At P7–P8, the hard pancreas of PKC mice invaded and adhered to the intestine, and mice died with massive ascites. However, we did not observe any metastasis in other organs. The P4 PKC mouse pancreas contained abundant stromal

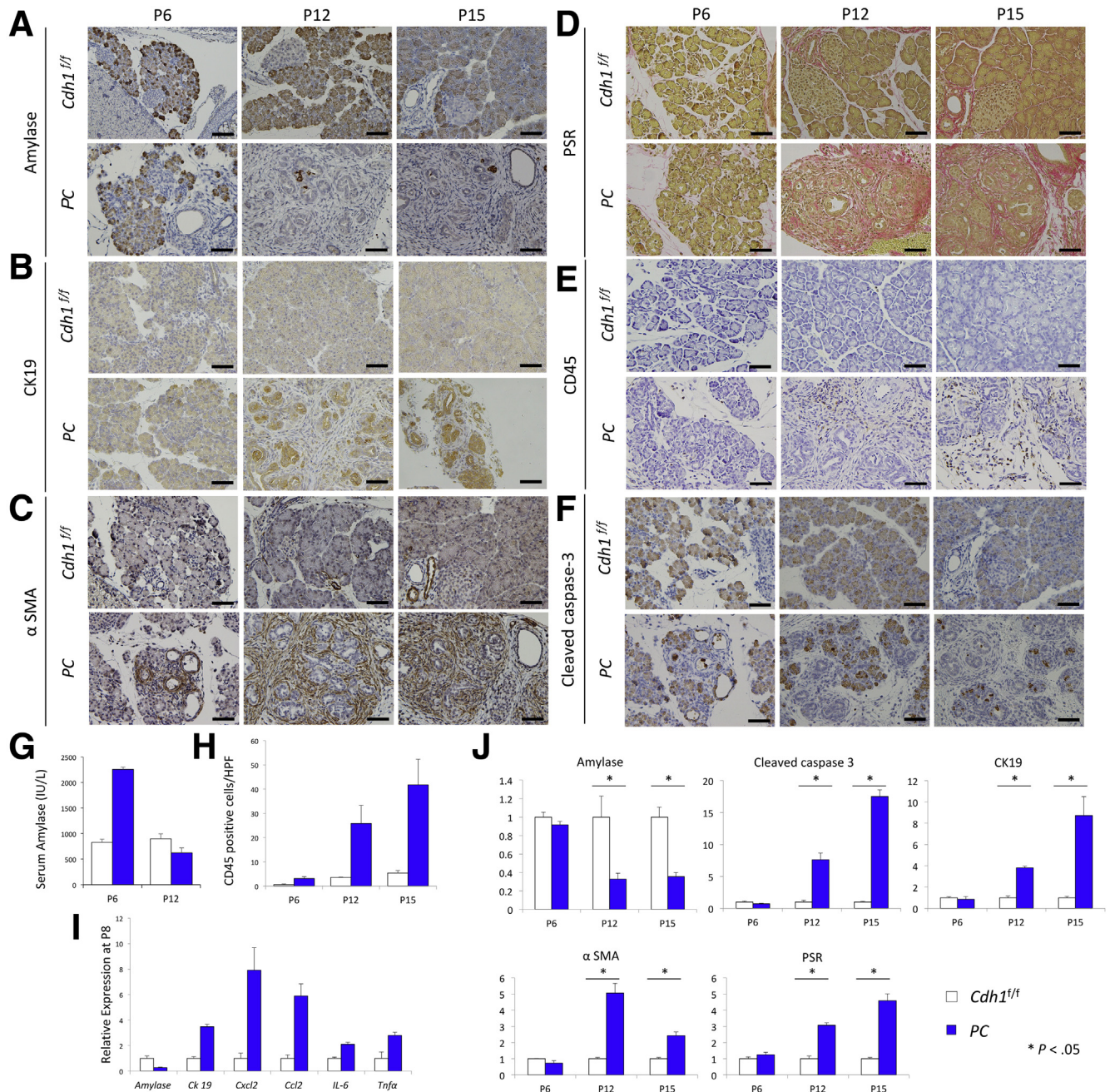


Figure 2. Genetic inactivation of *Cdh1* caused pancreatitis-like changes. IHC analysis of the *Cdh1^{fl/fl}* and PC pancreas on P6–P15 showed staining for (A) amylase, (B) CK19, (C) α -SMA, (D) PSR, (E) CD45, and (F) cleaved caspase-3 in the pancreas from mice of each genotype. (G) Serum amylase level of mice of each genotype on P6 and P12. (H) Quantification of CD45-positive cells per high-power field showed an increasing number of CD45-positive cells in the PC pancreas compared with the *Cdh1^{fl/fl}* pancreas. (I) Relative mRNA expression levels of amylase, CK19, inflammatory cytokines, and chemokines from pancreatic tissues of *Cdh1^{fl/fl}* and PC mice on P8. (J) Quantification of the area of positivity for amylase, cleaved caspase-3, CK19, α -SMA, and PSR at P6 and P15 in the pancreas of PC mice compared with wild-type mice (*Cdh1^{fl/fl}*). Scale bar: 100 μ m. * $P < .05$.

components that showed positive staining for α -SMA and vimentin (Figure 3E).

To characterize these components, we crossbred PKC mice with *Rosa26-LSL-tdTomato*. *Ptf1a-Cre* recombinant cells were labeled with *tdTomato* and confirmed by staining with red fluorescent protein (RFP). All PanINs and approximately half of the cells in stromal components were positive for RFP, suggesting that not only PanINs

but also many stromal cells were recombined with *Kras^{G12D/+}*. In addition, these lesions were positive for Ki67 and phospho-extracellular signal-regulated kinase (p-ERK). These results indicated that PKC stromal components contained tumor cells causing EMT with aggressive and invasive phenotypes (Figure 4A). We also performed immunofluorescence staining for RFP and CD44. Because RFP-positive cells and CD44-positive cells

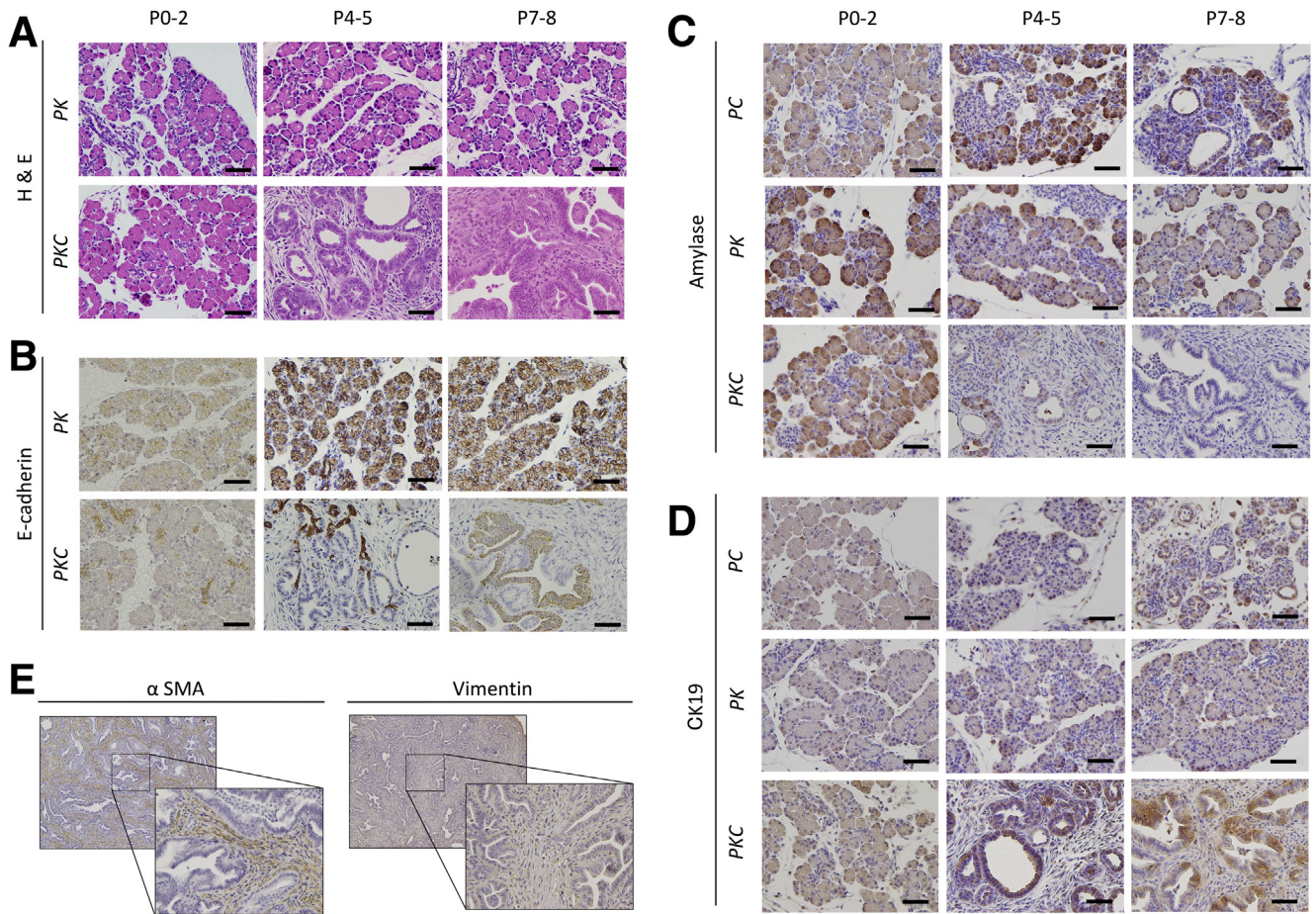


Figure 3. Loss of E-cadherin with mutational activation of *Kras* causes the formation of PanIN structures with desmoplastic reaction-like changes. (A) H&E staining of the pancreas from PK and PKC mice on P0–P8. IHC analysis of (B) E-cadherin, (C) amylase, and (D) CK19 in mice of the indicated genotypes and at the indicated time points. (E) The P8 PKC pancreas showed positive IHC staining for α -SMA and vimentin in stroma.

co-stained with some spindle-shaped cells, some of the cells undergoing recombination were likely to have had increased tumorigenic activity (Figure 4B). To investigate the changes caused by loss of E-cadherin, we evaluated DNA damage. Staining with γ histone 2AX (γ H2AX) was performed to assess DNA double-strand breaks. Although strongly positive nuclei were observed in PC mice, little staining was observed in PK mice. P4–P5 PKC mice showed slight positive staining, but the staining weakened at P7–P8 (Figure 4C). Similarly, cleaved caspase-3 was positive in PC, but in PKC the staining became weak (Figure 4D). ADM and PanIN lesions were mixed in the pancreas of PKC at P4. ADM lesions were positive for cleaved caspase-3, while PanIN lesions were negative (Figure 4E). To assess the extent of DNA damage, we quantified by IHC the proportions of cells positive for cleaved caspase-3 and γ H2AX (Figure 4F). Chemotherapy and radiotherapy are mainly responsible for DNA damage, but previous studies have shown that cells expressing oncogenic *Kras*^{G12D/+} acquired resistance through stem cell conversion.¹⁹ When pancreatic tissues of PKC were evaluated by quantitative reverse-transcription PCR, the levels of *Cd44*, Krüppel-like

factor 4 (*Klf4*), *Klf5*, and *Cd133* mRNA expression as markers of stem cells were increased compared with wild-type (Figure 4G). Cells positive for CD44, KLF4, and KLF5 on IHC were seen in the PKC pancreas, especially PanIN lesions (Figure 4H). These observations suggested that loss of E-cadherin provided tumorigenic activity to pancreatic cells and contributed to PanIN formation.

Establishment of Pancreatic Organoids From *Cdh1* Knockout Mice

To elucidate further the molecular mechanisms underlying the functions of E-cadherin, we established organoids derived from the pancreas of Cre-negative *Cdh1*^{fl/fl}, *LSL-Kras*^{G12D/+}, *LSL-Kras*^{G12D/+}; *Cdh1*^{fl/fl} mice, and induced Cre-recombination using lentivirus (see the Materials and Methods section) (corresponding to PC, PK, and PKC organoids, respectively). Loss of E-cadherin and expression of oncogenic *Kras*^{G12D/+} were confirmed by Western blot and IHC (Figure 5A and B). PC organoids represented the collapsed form, while other organoids showed a spherical shape. PK and PKC organoids, expressing oncogenic *Kras*^{G12D/+}, had dysplastic tall

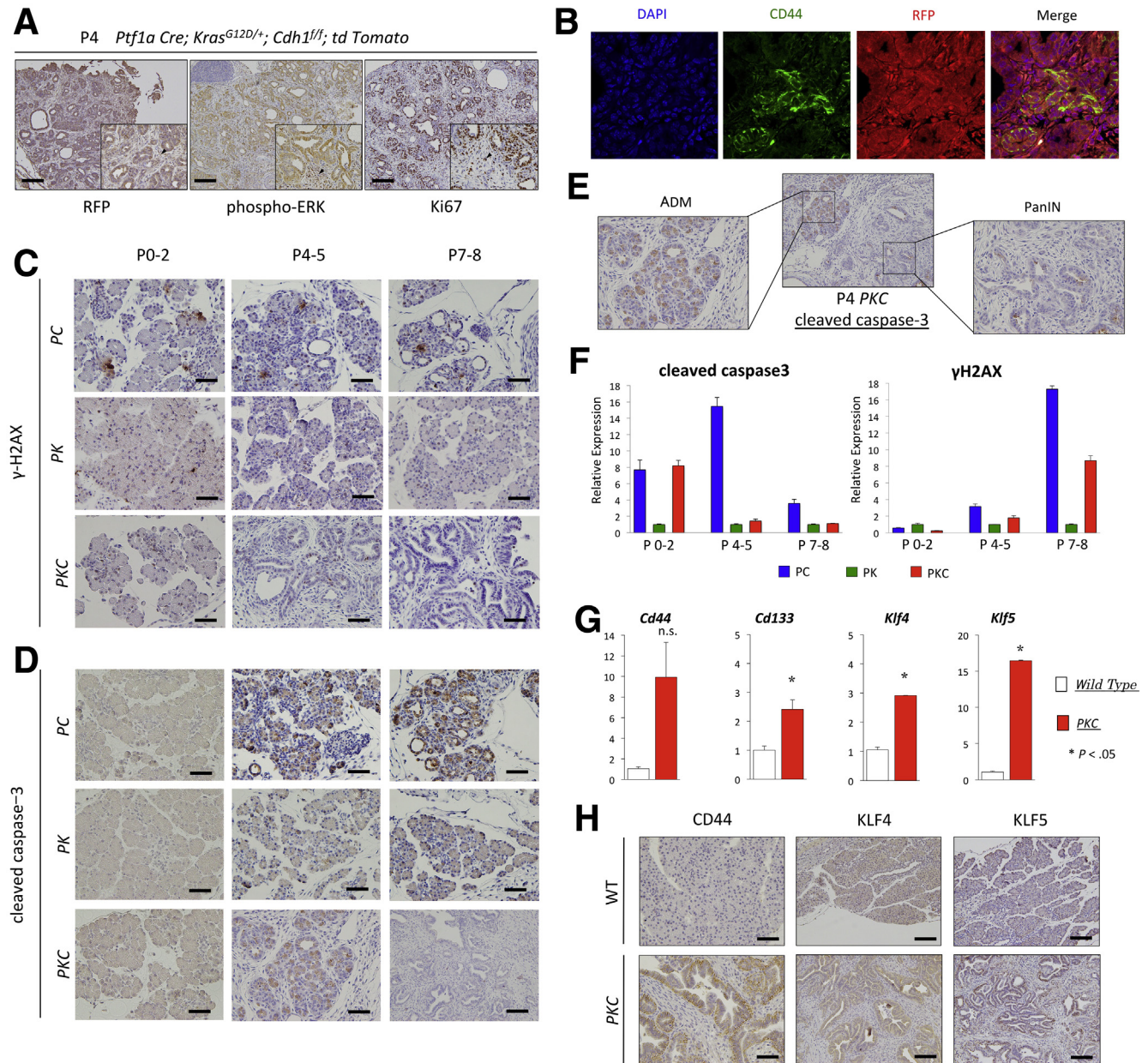


Figure 4. Loss of E-cadherin with mutational activation of *Kras* contributed to carcinogenesis. (A) IHC analysis for RFP, p-ERK, and Ki67 of PKC with *td Tomato* at P4. *Black arrowheads*: positive staining cells in stroma. (B) Immunofluorescence for RFP (red), CD44 (green), and 4',6-diamidino-2-phenylindole (DAPI) (blue) in the PKC pancreas at P4. IHC analysis of (C) γ H2AX and (D) cleaved caspase-3 from mice of the indicated genotypes and time points. (E) ADM structures showed positive IHC staining for cleaved caspase-3, whereas PanIN structures in the PKC pancreas at P4 showed mild positivity. (F) Quantification of the cleaved caspase-3- and γ H2AX-positive area in the P0-P2, P4-P5, and P7-P8 pancreas of PC and PKC mice compared with PK mice. (G) Relative mRNA expression levels of *Cd44*, *Klf4*, *Klf5*, and *Cd133* in pancreatic tissues of wild-type and PKC mice on P8. (H) IHC analysis of CD44, KLF4, and KLF5 from wild-type (WT) and PKC mice. Scale bar: 100 μ m.

columnar cells. PC organoids contained many cleaved caspase-3-positive cells, whereas PKC showed only partial positivity for caspase-3. These results were consistent with the in vivo data. Although loss of E-cadherin caused disruption of the morphology owing to apoptosis, addition of oncogenic *Kras^{G12D/+}* reversed that effect (Figure 5B). *Cdh1* was re-expressed using lenti-*Cdh1* in PKC organoids (PKC+C). PKC+C organoids showed aligned structures similar to the original PK organoids (Figure 5C).

E-cadherin expression was confirmed by Western blot (Figure 5D). We compared the expression of EMT markers (*Snail* and *Twist*) in PKC and PKC+C RNA samples to determine whether cadherin was caused by EMT because the levels of EMT markers did not differ significantly between the 2 types of samples (Figure 5E). Immunofluorescence analysis showed E-cadherin and β -catenin costaining in the cell wall in PKC+C. In contrast, β -catenin staining was observed in the cytoplasm in PKC organoids,

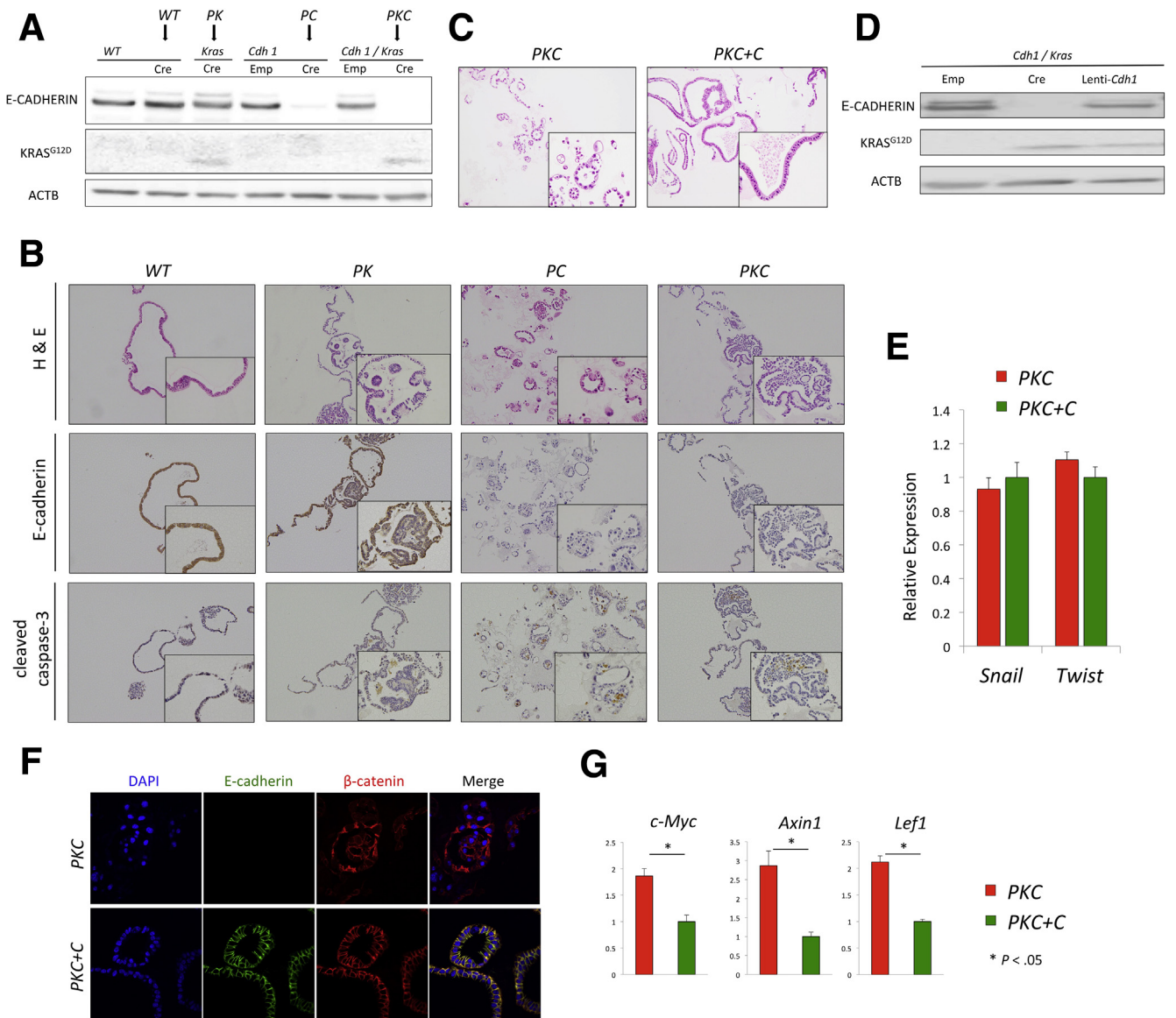


Figure 5. Establishment of pancreatic organoids expressing each genotype. (A) Confirmation of Cre-recombination using lentivirus by Western blot. ACTB (beta actin) served as loading control. Cre indicates lentivirus infection expressing cre recombinase and Emp indicates control lentivirus infection. (B) H&E and IHC staining for E-cadherin and cleaved caspase-3 in pancreatic organoids after gene recombination. (C) H&E staining of PKC and PKC+C (*Cdh1* re-expressing) organoids. (D) Confirmation of Cre-recombination and lentivirus-mediated *Cdh1* re-expression by Western blot. (E) Relative mRNA levels of *Snail* and *Twist* in PKC and PKC+C organoids. (F) Immunofluorescence staining for β -catenin (red), E-cadherin (green), and 4',6-diamidino-2-phenylindole (DAPI) (blue) of PKC and PKC+C organoids. (G) Relative mRNA levels of *c-Myc*, *Axin1*, and *Lef1* in PKC and PKC+C organoids. WT, wild-type.

suggesting increased Wnt signaling activity (Figure 5F). To examine Wnt signaling activity, we evaluated the mRNA levels of *c-Myc*, *Axin1*, and *Lef1*, which were higher in PKC compared with PKC+C (Figure 5G).

Cdh1-Deficient Cell Line With *Kras* Mutation Showed Greater Migratory and Invasive Activity

PC, PK, and PKC organoids were transplanted subcutaneously into nude mice to evaluate carcinogenesis. After 4 weeks, PK and PKC organoids formed tumors, whereas none (0 of 4) of the PC organoids formed tumors.

E-cadherin-positive ductal structures were found in PK tumors but disappeared in PKC tumors, and PKC tumors had structures similar to poorly differentiated adenocarcinoma according to the World Health Organization classification (Figure 6A and B). Evaluation of mesenchymal cells by IHC for vimentin showed partial positivity in PK, but extensive positivity in PKC (Figure 6C). We also examined liver metastasis by injecting these cells into the spleen. Liver metastases were induced successfully by both PK and PKC cells, but tumor number and size did not differ in the cell types. Tumor histology was consistent with the allograft model, and ductal structures were found in PK tumors but

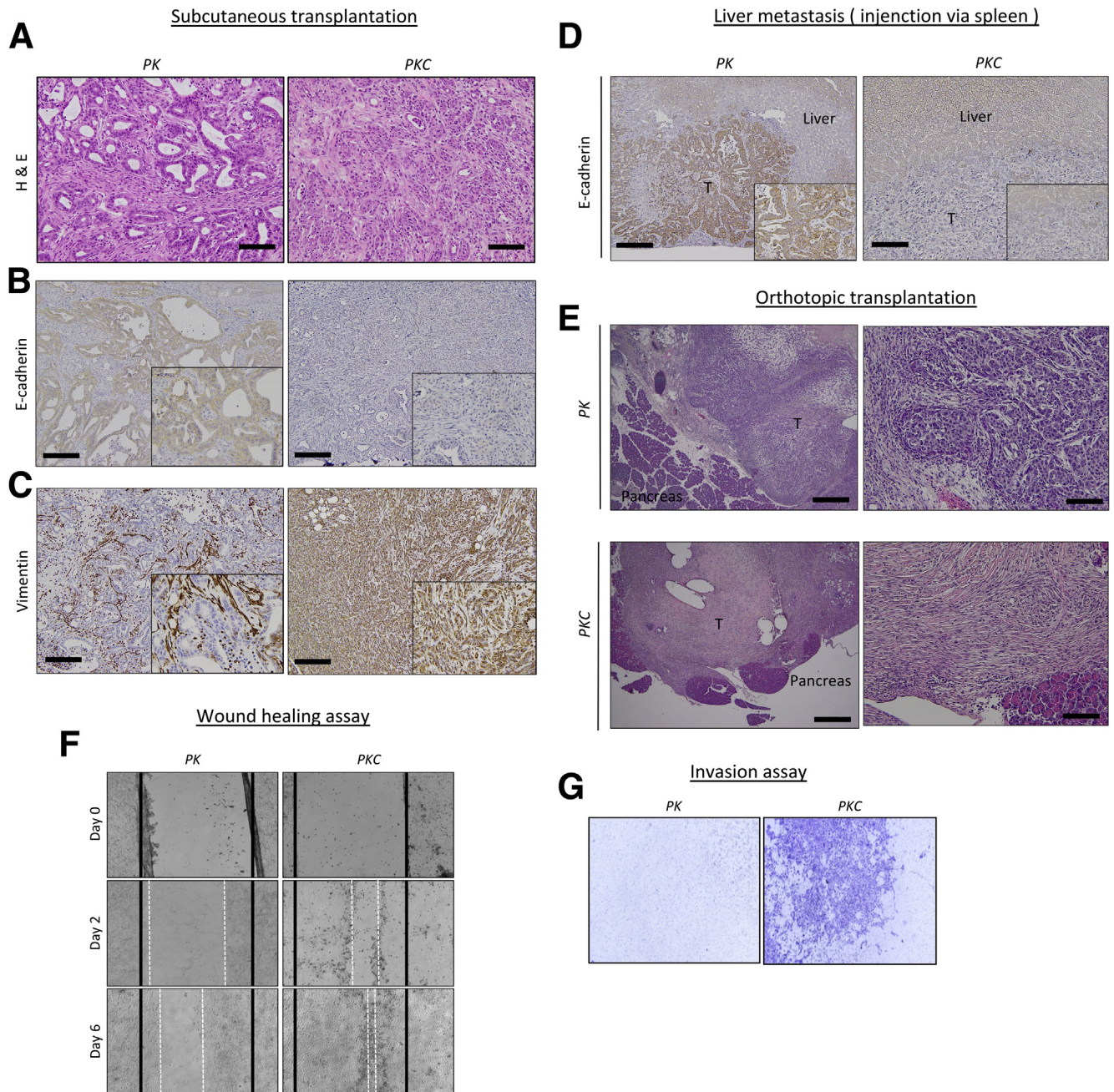


Figure 6. *Cdh1* deletion resulted in mesenchymal features with acquisition of migratory and invasive properties. Subcutaneous transplants from *PK* and *PKC* organoids were evaluated by staining with (A) H&E and for (B) E-cadherin and (C) vimentin. (D) *PKC* cells in liver metastases also lacked E-cadherin. IHC analysis of E-cadherin in liver metastatic allografts of *PK* and *PKC* mice. T indicates tumor. (E) H&E staining to confirm orthotopic transplantation of *PK* and *PKC* cells. (F) Wound healing assay showed that *PKC* cell lines had increased migratory ability compared with *PK* cell lines on days 2 and 6. (G) Invasion assay showed staining of greater numbers of *PKC* cells than *PK* cells.

not in *PKC* tumors. We also generated an orthotopic transplant model in which cells were injected into the pancreas, which had similar tissue types to the liver metastasis model (Figure 6D and E). Therefore, 2-dimensional (2D) culture was possible for *PK* and *PKC*, and we performed functional evaluation. Comparison of *PKC* with *PK* lines showed that loss of E-cadherin was associated with faster closure in a wound healing assay (Figure 6F) and greater invasive capability in an invasion assay (Figure 6G). These results

suggested that loss of E-cadherin significantly accelerates genetically induced pancreatic tumor formation through induction of EMT.

Loss of E-Cadherin in the Mature Pancreas Accelerates PanIN Formation

The mouse model described earlier was not suitable for long-term analysis of early death. Therefore, we

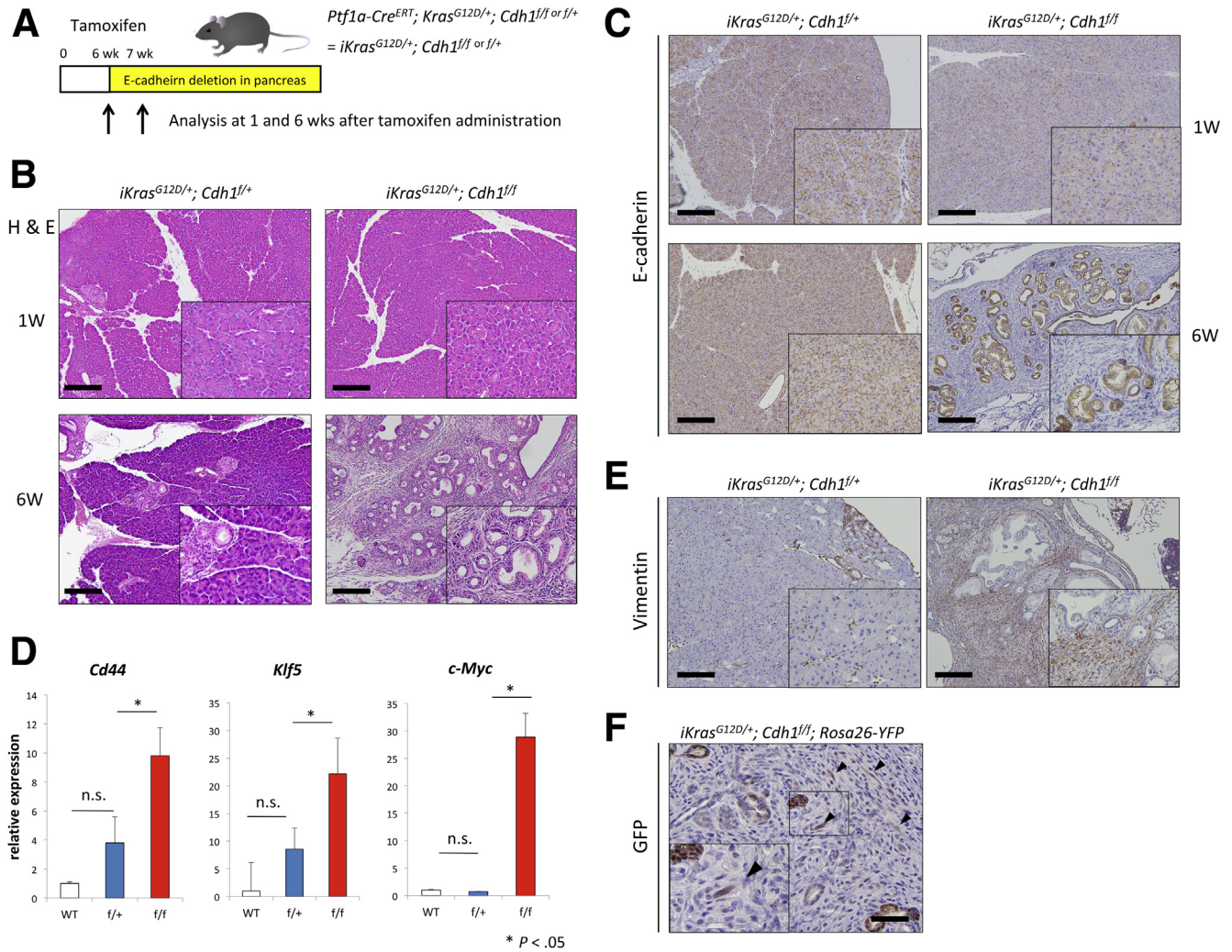


Figure 7. Loss of E-cadherin in the mature pancreas. (A) Protocol of E-cadherin deletion in the pancreas. (togoTV mouse images were used) (B) H&E staining and (C) IHC analysis for E-cadherin in mice of the indicated genotypes and at various time points. (D) Relative mRNA expression levels of *Cd44*, *Klf5*, and *c-Myc* in pancreatic tissues from mice of each genotype at 6 weeks after tamoxifen administration. WT, Cre-negative mice, *f/+*, *iKras^{G12D/+}; Cdh1^{f/+}*, *f/f*, *iKras^{G12D/+}; Cdh1^{f/f}*. (E) IHC analysis for vimentin showed desmoplastic reaction in the *iKras^{G12D/+}; Cdh1^{f/f}* pancreas, but not in *iKras^{G12D/+}; Cdh1^{f/+}* at 6 weeks after tamoxifen administration. (F) IHC analysis for green fluorescent protein (GFP) in mice of *iKras^{G12D/+}; Cdh1^{f/f}; Rosa26-YFP* at 6 weeks after tamoxifen administration. *Black arrowheads*: positive staining cells in the stroma. W, week; WT, wild-type.

generated a mouse model using the tamoxifen-inducible Cre recombination system. Tamoxifen was administered orally at 6 weeks of age, and the same amount was administered again 1 week later. Analysis was performed 1 and 6 weeks after tamoxifen administration (Figure 7A). We compared *Ptfla-Cre^{ERT}; Kras^{G12D/+}; Cdh1^{f/f}* (*iKras^{G12D/+}; Cdh1^{f/f}*) with *Ptfla-Cre^{ERT}; Kras^{G12D/+}; Cdh1^{f/+}* (*iKras^{G12D/+}; Cdh1^{f/+}*) because *Cdh1* heterodeficiency did not contribute to the phenotype (Figure 7B). There were no phenotypic changes in either mouse line at 1 week after tamoxifen administration. At 6 weeks, PanIN formation and desmoplastic reaction were observed in *iKras^{G12D/+}; Cdh1^{f/f}* (Figure 7B). Acini disappeared in *iKras^{G12D/+}; Cdh1^{f/f}*, and E-cadherin was positive only in the ductal part (Figure 7C). Even in these mouse models, the levels of *Cd44* and *Klf5* mRNA expression were increased, as in PKC

mice. In addition, the mRNA level of *c-Myc* was increased (Figure 7D), which may explain activation of Wnt signaling and is similar to the results in Figure 5F and G. The *iKras^{G12D/+}; Cdh1^{f/f}* stroma showed strongly positive staining for vimentin on IHC (Figure 7E). Next, we crossbred *iKras^{G12D/+}; Cdh1^{f/f}* mice with *Rosa26-LSL-yellow fluorescent protein (YFP)* (*iKras^{G12D/+}; Cdh1^{f/f}; Rosa26-YFP*) to allow lineage tracing of stromal cells. In this model, YFP was expressed in cells with functional Cre-recombinase and confirmed by IHC for green fluorescent protein staining. When Cre-recombination was caused by administration of tamoxifen, green fluorescent protein-positive cells were observed in stroma, but the proportion of positive cells was relatively small compared with cells of PKC mice. It was considered that the cells expressing *Ptfla* had

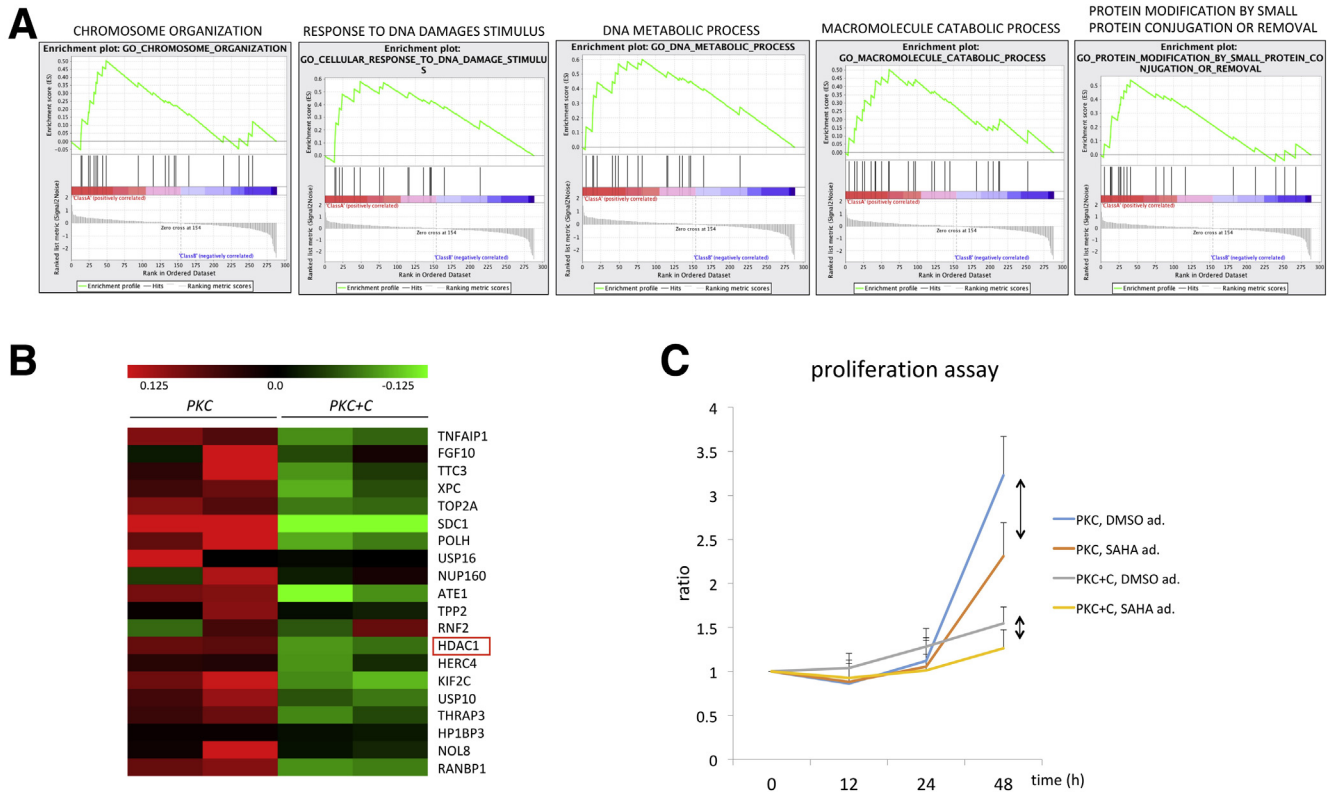


Figure 8. The presence of *Cdh1*-regulated *Hdac1*. (A) Gene set enrichment analysis of expressed genes from cDNA microarrays of PKC and PKC+C (nominal P value $< .05$). (B) Expression data of the top 20 genes showing differences in expression between PKC and PKC+C. (C) Proliferation assay for PKC and PKC+C with or without HDAC inhibitor (SAHA) ad, addition; DMSO, dimethyl sulfoxide.

morphologically changed into spindle-shaped cells (ie, tumor cells) with EMT (Figure 7F, black arrowheads).

Cdh1 Deletion Increases *Hdac1* Expression in PKC Cell Lines

Both PKC and PKC+C were subjected to complementary DNA (cDNA) microarray analysis. Analysis of the data with gene set enrichment analysis showed differences (nominal $P < .05$) in sets of genes, such as those involved in DNA damage and chromosome organization (Figure 8A). The top 20 up-regulated genes in PKC compared with PKC+C were extracted. We focused on *Hdac1* (Figure 8B) because histone deacetylase (HDAC) inhibitors have been reported to be effective in pancreatic cancer cells.²⁰ To investigate the contribution of *Cdh1* deficiency to its effect, we performed a proliferation assay using cells grown in 2D culture. PKC cells had a higher proliferative capacity than PKC+C, but a significant growth inhibitory effect of HDAC inhibitor (SAHA) was observed in PKC cells (Figure 8C). These results suggest that *Hdac1* might be a therapeutic target for cells with E-cadherin deletion.

Discussion

The results of the present study show the roles of *Cdh1* in a pancreas-specific conditional knock-out mouse model. In the physiological state, loss of E-cadherin resulted in the

disappearance of acinar cells and the formation of ducts with apoptotic changes, suggesting a phenotype of pancreatitis-like changes based on evaluation of serum amylase levels, CD45-positive cells, and inflammatory cytokines. Pancreatitis-like changes are caused by the increased levels of proinflammatory cytokines at P8 and the serum level of amylase at P6. In contrast, the serum amylase level and the number of IHC-positive cells were decreased at P12. In addition, the number of caspase-3, IHC-positive cells was greater at P15 compared with P6. Therefore, loss of E-cadherin causes tissue disruption and induces pancreatitis-like changes, followed by death at approximately P28 because of functional failure of the pancreas. In vitro, organoids could not maintain epithelial alignment, indicating a direction in which apoptosis was induced as in vivo. Previously, we reported that loss of E-cadherin in the intrahepatic bile duct epithelium functionally impaired biliary flow, and subsequently induced cholestatic liver injury and sclerosing cholangitis.⁴ We assumed that E-cadherin plays an important role in maintaining cell-to-cell contact in the pancreatic duct and that loss of E-cadherin impairs the flow of pancreatic juice and eventually causes pancreatitis-like changes. Similar mouse data were published during preparation of this manuscript, although no organoids and human data have been reported.²¹ Consistent with previous studies, even in the pancreas, E-cadherin deficiency alone did not induce carcinogenesis.^{4,22,23} Mutational *Kras* activation was

found in human pancreatic cancer at a frequency of 90%,¹⁶ and mutational *Kras* activation was also an important genetic mutation in a mouse model.²⁴ In the mouse model, the frequency of carcinogenesis induced only by *Kras* mutation was low, and the incidence of carcinogenesis increased with the addition of dysfunction of cancer-suppressing genes, such as *p53* and *Ink4a/Arf*.^{17,25,26} When *Cdh1*-deficient mice were subjected to mutational *Kras* activation (PKC mice), histologic changes in the direction of tumor formation were observed in the early postnatal stage, whereas *Kras* activation alone resulted in no morphologic changes (PK mice). This model showed the formation of PanIN and increased stroma resembling aggressive tumors. In our studies using *td Tomato* reporter mice, RFP-positive cells were observed in the stroma. In addition, cells positive for p-ERK and Ki67 were observed in the stroma, suggesting the occurrence of massive neoplastic growth in the stroma. The co-staining of RFP and CD44 indicates that those cells have acquired tumorigenic activity.

E-cadherin is considered to act as a tumor suppressor,²⁷ and mutation of its gene contributes to carcinogenesis. In gastric and breast cancer, *Cdh1* deficiency and mutation are observed at a certain frequency.^{28,29} Low E-cadherin expression level has been reported in pancreatic cancer,⁷ but *Cdh1* deficiency and mutation are uncommon.³⁰ Therefore, the role of E-cadherin in pancreatic cancer still is unclear. The mouse model produced in this study combined the deficiency of E-cadherin and mutational *Kras* activation in the pancreas. This model showed PanIN formation and increased stroma resembling aggressive tumors at an early stage after birth. Our studies using *td Tomato* and *YFP* reporter mice indicated the presence of cells derived from *Ptfla-Cre* in the stroma,^{31,32} and cells positive for p-ERK and Ki67 were observed in the stroma. These observations suggest the occurrence of neoplastic growth. Because these model mice die approximately 10 days after birth, evaluation of the tumors themselves was difficult. Therefore, we produced a tamoxifen-inducible mouse model. Mutational *Kras* activation and *Cdh1* deficiency were introduced in the mature pancreas. This transgenic mouse model showed PanIN formation, which takes half a year with *Kras* mutation alone,¹⁷ within the entire pancreas at approximately 6 weeks of age.

The observations of the present study raise questions as to why tumor formation occurs more quickly in the E-cadherin deletion model. One possibility is that compensatory proliferation after cell death owing to E-cadherin deletion may play an important role in transformed cell proliferation. Previously, we reported that the death of parenchymal cells activated adjacent myeloid cells to produce mitogens that promote compensatory proliferation of surviving transformed parenchymal cells to liver carcinogenesis.³³ However, we saw only a small amount of cell death in the model, whereas proliferative response and mitogenic cytokine levels were increased. Alternatively, deletion of E-cadherin may confer tumorigenic activity and cause cellular reprogramming, resulting in tumor initiation.³⁴ Recent reports have suggested that the transient expression of reprogramming factors in *Kras* mutant mice is sufficient to induce the activation of ERK signaling in acinar

cells and rapid formation of PDAC.³⁵ Notably, we found that expression levels of *Cd44*, *Klf4*, *Klf5*, and *Cd133*, markers of stem cells or reprogramming, were increased in PKC tumor tissues. High *Cd44* expression level is correlated with poor prognosis and poorly differentiated phenotype in human PDAC.^{36–38} *Klf4* and *Klf5* also are expressed in pancreatic cancer and have been reported to be an important transcription factor for PanIN formation.^{39,40} The increased mRNA level of *c-Myc* in *iKras*^{G12D/+}; *Cdh1*^{fl/fl} pancreatic tissue indicates promotion of Wnt-induced growth signaling pathways. In the organoids of the PKC mice, β -catenin was transferred to the cytoplasm and the mRNA levels of *c-Myc*, *Axin1*, and *Lef1*, which are markers of Wnt signaling, were increased in comparison with those of the PKC+C mice. Structurally, E-cadherin and β -catenin are connected, and it is thought that Wnt signaling is activated by β -catenin in the absence of E-cadherin.² However, the precise mechanism by which deletion of E-cadherin increases the expression of these factors is unknown.

Another question is whether E-cadherin deletion in tumors causes EMT or a histologically undifferentiated phenotype. In gastric cancer and breast cancer, *Cdh1*-deficient tumors often become poorly differentiated tissue.^{8,41} In the present study, allografts of *Cdh1*-deficient and *Kras* mutational tumors showed a tissue type similar to undifferentiated pancreatic cancer. E-cadherin-deficient tumor cells were positive for vimentin and showed high motility and invasiveness, suggesting that the cells had gained an EMT phenotype. However, we did not see an apparent increase in metastasis associated with E-cadherin deletion. These observations were consistent with a previous report that EMT may increase tumor invasiveness, but are not involved in tumor metastasis in vivo.⁴²

Although it is difficult to capture the target of a candidate treatment for tumors in E-cadherin deletion or reduced tumors, the results of our cDNA microarray analysis indicated that *Hdac1* was one of the targets. HDAC plays an important role in chromatin remodeling and controls transcription. The expression of HDAC is increased in tumors and suppresses the expression of tumor-suppressor genes by epigenetic control to deacetylate histones and therefore promotes tumor formation. HDAC inhibitor was reported to up-regulate a gene, the expression of which is suppressed by histone acetylation.⁴³ In pancreatic cancer, HDAC is increased and it has been reported that HDAC increase inhibits the expression of E-cadherin.⁴⁴ There have been no reports of increased HDAC expression resulting from the loss of E-cadherin in the pancreas and, therefore, further studies are required. We examined whether the presence or absence of E-cadherin in pancreatic cancer cells contributes to the effect of HDAC inhibition using an HDAC inhibitor, which already has been introduced in a clinical trial in pancreatic cancer.⁴⁵ The results indicated that *Cdh1* knockout cells had more aggressive proliferative behavior, but the inhibition rate by HDAC inhibitor was greater than that in the presence of *Cdh1*, and so loss of E-cadherin may be a predictive marker for the effectiveness of HDAC inhibitor treatment. In clinical trials, HDAC inhibitors have not been used in combination with key drugs such as

gemcitabine, and so further trials are warranted. In addition, although the effect of HDAC inhibitors on E-cadherin deficiency has been reported, the presence of a variety of genetic mutations reduces their efficacy in clinical practice.⁴⁴ In this study, we used a model in which E-cadherin was deleted and *Kras* was mutated, and so the effect of the HDAC inhibitor may have resulted from the lower grade of malignancy compared with human pancreatic cancer.

In summary, E-cadherin is important for maintenance of homeostasis in the pancreas. Under pathologic conditions with mutational *Kras* activation, E-cadherin plays an important role in tumor formation via acquisition of tumorigenic activity. Loss of E-cadherin is associated with an increase in *Hdac1* expression, and *Cdh1*-negative patients may show a greater beneficial effect of HDAC inhibitor treatment.

Materials and Methods

Mice

Ptf1a-Cre, *LSL-Kras*^{G12D/+}, *Ptf1a-Cre*^{ERT}, *Cdh1*^{l/f}, and *Rosa26-LSL-tdTomato* mice were described previously.^{17,21,31,46,47} Nude mice were purchased from CLEA (Tokyo, Japan). The mice were maintained at the Institute for Adult Diseases of the Asahi Life Foundation and the Graduate School of Medicine of Yokohama City University. The Ethics Committees for Animal Experimentation of Yokohama City University and the Institute for Adult Diseases of the Asahi Life Foundation approved all experiments involving animals.

Organoid Experiments

Isolated pancreatic tissue was minced and digested in dissociation medium consisting of Dulbecco's modified Eagle medium (DMEM) supplemented with 1% fetal bovine serum and 5 mg/mL collagenase II (Sigma, St. Louis, MO). Next, pancreatic tissue was mixed with Matrigel (Corning) and seeded onto plates containing culture medium consisting of Advanced DMEM/F12 (Gibco, Waltham, MA) supplemented with 10 mmol/L 4-(2-hydroxyethyl)-1-piperazineethanesulfonic acid, B27, and N2, 10 mmol/L nicotinamide, 1 mmol/L *N*-acetylcysteine (Sigma), 50 ng/mL epidermal growth factor (Peprotech), 100 ng/mL fibroblast growth factor (Peprotech), 100 ng/mL Noggin (Peprotech, Rocky Hill, NJ), 10% R-spondin-1-conditioned medium, and 50% Wnt3A conditioned medium. The organoids were incubated in Cell Recovery Solution (BD Biosciences, Franklin Lakes, NJ) and embedded in Matrigel to be passaged.

To induce Cre recombination, organoids were infected with Cre-expressing lentiviral vectors and selected using puromycin. In addition, *Cdh1*-deleted organoids were infected with lenti-*Cdh1* to induce re-expression of CDH1, and were selected using hygromycin B.

Reagents

The HDAC inhibitor (SAHA, cat 10009929; Cayman Chemical, Ann Arbor, MI) was dissolved in dimethyl sulfoxide at 100 mmol/L and diluted to 1 μ mol/L. The primary antibodies used in these experiments were anti-E-cadherin, anticleaved caspase-3, anti-phospho-ERK, anti- γ H2AX, and

antivimentin (Cell Signaling, Beverly, MA); anti-Ki67, anti-amylase, and anti-CK19 (Abcam); anti- α -SMA (Santa Cruz Biotechnology, Santa Cruz, CA); anti-CD45 and anti- β -catenin (BD Biosciences); anti-RFP (Rockland Antibodies & Assays, Limerick, PA); and anti-green fluorescent protein (Medical & Biological Laboratories, Nagoya, Japan). Tamoxifen (Sigma) was dissolved in corn oil containing 10% ethanol and was administered by oral gavage to mice at 6 weeks of age (5 mg per mouse).

Histology

The pancreas was isolated from the mice and fixed in 10% formalin in phosphate buffer. Tissues were embedded in paraffin, cut into sections, mounted on slides, and subjected to staining with H&E or PSR, and processed for IHC. After deparaffinization and rehydration, the slides were incubated with 3% H₂O₂ at room temperature to block endogenous peroxidase activity. For antigen retrieval, the slides were incubated for 15 minutes at 121°C in an autoclave or twice for 10 minutes each in a microwave oven at 600 W, and subsequently incubated overnight at 4°C with the indicated primary antibodies. Biotinylated anti-rabbit, anti-rat, and anti-mouse secondary antibodies (1:200 dilution; Vector Laboratories, Burlingame, CA) were next added for 30 minutes at room temperature. The solutions in the Vectastain ABC Kit (Vector Laboratories) diluted 1:200 were applied to the slides in accordance with the manufacturer's directions. After 30 minutes, the slides were developed with 3,3'-diaminobenzidine substrate (Muto Pure Chemicals, Tokyo, Japan) and counterstained with hematoxylin. The area of staining was quantitated using ImageJ software (National Institutes of Health, Bethesda, MD). For immunofluorescence, slides were incubated with the indicated primary antibodies, followed by the corresponding secondary antibodies labeled with Alexa 488 or 594 (Molecular Probes, Eugene, OR). After 30 minutes, the slides were mounted with 4',6-diamidino-2-phenylindole (Vector Laboratories).

Western Blot

Whole-pancreas protein homogenates and cell lysates prepared using Tissue Protein Extraction Reagent (Thermo Fisher Scientific) were subjected to sodium dodecyl sulfate-polyacrylamide gel electrophoresis and transferred onto Immobilon-P membranes (Merck Millipore). The membranes were incubated in polyvinylidene difluoride blocking reagent (Toyobo) for 1 hour and subsequently overnight at 4°C with the indicated primary antibodies. Next, the membranes were incubated with the appropriate secondary antibodies, and immune complexes were detected using the ECL Prime Western Blotting Detection Reagent (GE Healthcare). Images were obtained using an LAS-3000 (Fujifilm) or ChemiDoc (Bio-Rad) imaging system.

Quantitative Reverse-Transcription PCR

RNA was extracted from pancreatic tissue using ISO-GEN2 (Nippon Gene, Tokyo, Japan), and cDNA was generated using a High-Capacity RNA-to-cDNA Kit (Thermo Fisher

Scientific). Quantitative reverse-transcription PCR was performed using Fast SYBR Green Master Mix (Thermo Fisher Scientific) and a 7900HT Fast Real-Time PCR System (Applied Biosystems, Foster City, CA). Gene expression levels were normalized to that of *GAPDH* as an internal reference. Primer sequences are available upon request.

Cell Culture

We established *Ptf1a^{cre/+}; Kras^{G12D/+}; Cdh1^{fl/fl}* (PKC) and *Ptf1a^{cre/+}; Kras^{G12D/+}*, re-expressing *Cdh1* (PKC+C) 2D cell lines from the organoids using the lentiviral vectors described earlier in DMEM (Gibco) containing 10% fetal bovine serum (Biosera, Nuaille, France), and 2% penicillin-streptomycin (Thermo Fisher Scientific). *Ptf1a^{cre/+}; Cdh1^{fl/fl}* organoids could not be established in 2D culture.

Subcutaneous Tumor and Liver Metastasis Allograft Models

For the allograft model, centrifuged organoid fragments were injected subcutaneously into nude mice. Tumors were removed and measured when they became palpable. For the liver metastasis model, we prepared 2D-cultured cells from the organoids. The prepared cells were injected into the spleen using a 29-gauge needle. To prevent tumor-cell leakage, a cotton swab was held over the spleen for 1 minute. The splenic blood vessels were ligated, the injected spleen was removed, and the wound was sutured with clips.

Wound Healing Assay

Mouse cancer cells were seeded onto 6-well plates and starved of serum overnight when near complete confluence. Next, scratch wounds (500 μm) were made using a cover glass. The cells were incubated for up to 6 days and migration was assessed at the indicated time points.

Invasion Assay

Invasion was assayed using a commercial kit (BioCoat Matrigel Invasion Chamber; BD Biosciences), which contains polyethylene terephthalate membrane inserts with a pore size of 8.0 μm in a 24-well format, according to the manufacturer's protocol.

Cell Proliferation Assay

Aliquots of 6×10^3 PKC or PKC+C cells were seeded onto 48-well plates and incubated for 24 hours. The culture medium was removed and fresh medium containing dimethyl sulfoxide or SAHA was added. Next, 10 μL of Cell Counting Kit-8 (Dojindo, Tokyo, Japan) solution was added to each well and the culture medium was transferred to 96-well plates for measurement of the absorbance at 450 nm using a microplate reader (Beckman Coulter, Brea, CA) at 0, 12, 24, and 48 hours.

Microarray

The SurePrint G3 Mouse Gene Expression $8 \times 60\text{K}$ v2 (Agilent Technologies, Santa Clara, CA) microarray was

used in this study according to the manufacturer's protocol. The microarray data were subjected to gene set enrichment analysis with permutations across gene sets using the c5.all.v6.2.symbols.gmt gene sets from the Molecular Signatures Database.

Statistical Analysis

Values are presented as means \pm SEM. The significance of differences was examined using the Student *t* test. In all analyses, $P < .05$ indicated statistical significance.

References

1. Takeichi M. Dynamic contacts: rearranging adherens junctions to drive epithelial remodelling. *Nat Rev Mol Cell Biol* 2014;15:397–410.
2. Halbleib JM, Nelson WJ. Cadherins in development: cell adhesion, sorting, and tissue morphogenesis. *Genes Dev* 2006;20:3199–3214.
3. Larue L, Ohsugi M, Hirchenhain J, Rolf Kemler. E-cadherin null mutant embryos fail to form a trophoblast epithelium. *Proc Natl Acad Sci U S A* 1994;91:8263–8267.
4. Nakagawa H, Hikiba Y, Hirata Y, Font-Burgada J, Sakamoto K, Hayakawa Y, Taniguchi K, Umemura A, Kinoshita H, Sakitani K, Nishikawa Y, Hirano K, Ikenoue T, Ijichi H, Debanjan D, Shibata W, Akanuma M, Koike K, Karin M, Maeda S. Loss of liver E-cadherin induces sclerosing cholangitis and promotes carcinogenesis. *Proc Natl Acad Sci U S A* 2014;111:1090–1095.
5. Nakada S, Tsuneyama K, Kato I, Tabuchi Y, Takasaki I, Furusawa Y, Kawaguchi H, Fujimoto M, Goto H, Hikiami H, Kondo T, Takano Y, Shimada Y. Identification of candidate genes involved in endogenous protection mechanisms against acute pancreatitis in mice. *Biochem Biophys Res Commun* 2010;391:1342–1347.
6. Lerch MM, Lutz MP, Weidernbach H, Pillasch FM, Gress TM, Leser J, Adler G. Dissociation and reassembly of adherens junctions during experimental acute pancreatitis. *Gastroenterology* 1997;113:1355–1366.
7. Deng S, Zhu S, Wang B, Li X, Liu Y, Qin Q, Gong Q, Niu Y, Xiang C, Chen J, Jin Y, Deng S, Yin T, Yang M, Wu H, Wang C, Zhao G. Chronic pancreatitis and pancreatic cancer demonstrate active epithelial-mesenchymal transition profile, regulated by miR-217-SIRT1 pathway. *Cancer Lett* 2014;355:184–191.
8. Becker KF, Atkinson MJ, Reich U, Becker I, Nekarda H, Siewert JR, Hofler H. E-cadherin gene mutations provide clues to diffuse type gastric carcinomas. *Cancer Res* 1994;54:3845–3852.
9. Oliveira C, Pinheiro H, Figueiredo J, Seruca R, Carneiro F. Familial gastric cancer: genetic susceptibility, pathology, and implications for management. *Lancet Oncol* 2015;16:e60–e70.
10. Hayakawa Y, Ariyama H, Stancikova J, Sakitani K, Asfaha S, Renz BW, Dubeykovskaya ZA, Shibata W, Wang H, Westphalen CB, Chen X, Takemoto Y, Kim W, Khurana SS, Tailor Y, Nagar K, Tomita H, Hara A, Seplveda AR, Setlik W, Gershon MD, Saha S, Ding L, Shen Z, Fox JG, Friedman RA, Konieczny SF,

- Worthley DL, Korinek V, Wang TC. Mist1 expressing gastric stem cells maintain the normal and neoplastic gastric epithelium and are supported by a perivascular stem cell niche. *Cancer Cell* 2015;28:800–814.
11. Kinoshita H, Hayakawa Y, Konishi M, Hara M, Tsuboi M, Hayata Y, Hikiba Y, Ihara S, Nakagawa H, Ikenoue T, Ushiku T, Fukuyama M, Hirata Y, Koike K. Three types of metaplasia models through Kras activation, Pten deletion, or Cdh1 deletion in the gastric epithelium. *J Pathol* 2019;247:35–47.
 12. Shimada S, Mimata A, Sekine M, Mogushi K, Akiyama Y, Fukamichi H, Jonkers J, Tanaka H, Eishi Y, Yuasa Y. Synergistic tumour suppressor activity of E-cadherin and p53 in a conditional mouse model for metastatic diffuse-type gastric cancer. *Gut* 2012;61:344–353.
 13. Siegel RL, Miller KD, Jemal A. Cancer statistics, 2017. *CA Cancer J Clin* 2017;67:7–30.
 14. Chen L, Ma C, Bian Y, Shao C, Wang T, Li J, Chong X, Su L, Lu J. Aberrant expression of STYK1 and E-cadherin confer a poor prognosis for pancreatic cancer patients. *Oncotarget* 2017;8:111333–111345.
 15. Lee JM, Dedhar S, Kalluri R, Thompson EW. The epithelial-mesenchymal transition: new insights in signaling, development, and disease. *J Cell Biol* 2006;172:973–981.
 16. Rozenblum E, Schutte M, Goggins M, Hahn SA, Panzer S, Zahurak M, Goodman SN, Sohn TA, Hruban RH, Yeo CJ, Kern SE. Tumor-suppressive pathways in pancreatic carcinoma. *Cancer Res* 1997;57:1731–1734.
 17. Hingorani SR, Petricoin EF, Maitra A, Rajapakse V, King C, Jacobetz MA, Ross S, Conrads TP, Veenstra TD, Hitt BA, Kawaguchi Y, Johann D, Liotta LA, Crawford HC, Putt ME, Jacks T, Wright CVE, Hruban RH, Lowy AM, Tuveson DA. Preinvasive and invasive ductal pancreatic cancer and its early detection in the mouse. *Cancer Cell* 2003;4:437–450.
 18. Shibata W, Kinoshita H, Hikiba Y, Sato T, Ishii Y, Sue S, Sugimori M, Suzuki N, Sakitani K, Ijichi H, Mori R, Endo I, Maeda S. Overexpression of HER2 in the pancreas promotes development of intraductal papillary mucinous neoplasms in mice. *Sci Rep* 2018;8:6150.
 19. Wang M, Han J, Marcar L, Black J, Liu Q, Li X, Nagulapalli K, Sequist LV, Mak RH, Benes CH, Hong TS, Gurtner K, Krause M, Baumann M, Kang JX, Whetstone JR, Willers H. Radiation resistance in KRAS-mutated lung cancer is enabled by stem-like properties mediated by an osteopontin-EGFR pathway. *Cancer Res* 2017;77:2018–2028.
 20. Cai MH, Xu XG, Yan SL, Sun Z, Ying Y, Wang BK, Tu YX. Depletion of HDAC1, 7 and 8 by histone deacetylase inhibition confers elimination of pancreatic cancer stem cells in combination with gemcitabine. *Sci Rep* 2018;8:1621.
 21. Serrill JD, Sander M, Shih HP. Pancreatic exocrine tissue architecture and integrity are maintained by E-cadherin during postnatal development. *Sci Rep* 2018;8:13451.
 22. Tinkle CL, Lechler T, Pasolli HA, Fuchs E. Conditional targeting of E-cadherin in skin: insights into hyperproliferative and degenerative responses. *Proc Natl Acad Sci U S A* 2004;101:552–557.
 23. Derksen PW, Liu X, Saridin F, van der Gulden H, Zevenhoven J, Evers B, van Beijnum JR, Griffioen AW, Vink J, Krimpenfort, Peterse JL, Cardiff RD, Berns A, Jonkers J. Somatic inactivation of E-cadherin and p53 in mice leads to metastatic lobular mammary carcinoma through induction of anoikis resistance and angiogenesis. *Cancer Cell* 2006;10:437–449.
 24. Herreros-Villanueva M, Hijona E, Cosme A, Bujanda L. Mouse models of pancreatic cancer. *World J Gastroenterol* 2012;18:1286–1294.
 25. Hingorani SR, Wang L, Multani AS, Combs C, Deramaudt TB, Hruban RH, Rustgi AK, Chang S, Tuveson DA. Trp53R172H and KrasG12D cooperate to promote chromosomal instability and widely metastatic pancreatic ductal adenocarcinoma in mice. *Cancer Cell* 2005;7:469–483.
 26. Aguirre AJ, Bardeesy N, Sinha M, Lopez L, Tuveson DA, Horner J, Redston MS, DePinho RA. Activated Kras and Ink4a/Arf deficiency cooperate to produce metastatic pancreatic ductal adenocarcinoma. *Genes Dev* 2003;17:3112–3126.
 27. Jeanes A, Gottardi CJ, Yap AS. Cadherins and cancer: how does cadherin dysfunction promote tumor progression? *Oncogene* 2008;27:6920–6929.
 28. Corso G, Carvalho J, Marrelli D, Vindigni C, Carvalho B, Seruca R, Roviello F, Oliveira C. Somatic mutations and deletions of the E-cadherin gene predict poor survival of patients with gastric cancer. *J Clin Oncol* 2013;31:868–875.
 29. Stuebs F, Heidemann S, Caliebe A, Mundhenke C, Arnold N. CDH1 mutation screen in a BRCA1/2-negative familial breast-/ovarian cancer cohort. *Arch Gynecol Obstet* 2018;297:147–152.
 30. Busch EL, Hornick JL, Umeton R, Albayrak A, Lindeman NI, MacConail LE, Garcia EP, Ducar M, Rebbeck TR. Somatic mutations in CDH1 and CTNNB1 in primary carcinomas at 13 anatomic sites. *Oncotarget* 2017;8:85680–85691.
 31. Madisen L, Zwingman TA, Sunkin SM, Oh SW, Zariwala HA, Gu H, Ng LL, Palmiter RD, Hawrylycz MJ, Jones AR, Lein ES, Zeng H. A robust and high-throughput Cre reporting and characterization system for the whole mouse brain. *Nat Neurosci* 2010;13:133–140.
 32. Nagai T, Ibata K, Park ES, Kubota M, Mikoshiba K, Miyazaki A. A variant of yellow fluorescent protein with fast and efficient maturation for cell-biological applications. *Nat Biotechnol* 2002;20:87–90.
 33. Maeda S, Kamata H, Luo JL, Leffert H, Karin M. IKKbeta couples hepatocyte death to cytokine-driven compensatory proliferation that promotes chemical hepatocarcinogenesis. *Cell* 2005;121:977–990.
 34. Skrypek N, Goossens S, De Smedt E, Vandamme N, Bex G. Epithelial-to-mesenchymal transition: epigenetic reprogramming driving cellular plasticity. *Trends Genet* 2017;33:943–959.
 35. Shibata H, Komura S, Yamada Y, Sankoda N, Tanaka A, Ukai T, Kabata M, Sakurai S, Kuze B, Woltjen K, Haga H, Ito Y, Kawaguchi Y, Yamamoto T, Yamada Y. In vivo

- reprogramming drives Kras-induced cancer development. *Nat Commun* 2018;9:2081.
36. Mani SA, Guo W, Liao MJ, Eaton EN, Ayyanan A, Zhou AY, Brooks M, Reinhard F, Zhang CC, Shipitsin Campbell LL, Polyak K, Brisken C, Yang J, Weinberg RA. The epithelial-mesenchymal transition generates cells with properties of stem cells. *Cell* 2018; 133:704–715.
 37. Hermann PC, Huber SL, Herrler T, Aicher A, Ellwart JW, Guba M, Bruns CJ, Heeschen C. Distinct populations of cancer stem cells determine tumor growth and metastatic activity in human pancreatic cancer. *Cell Stem Cell* 2007;1:313–323.
 38. Li XP, Zhang XW, Zheng LZ, Guo WJ. Expression of CD44 in pancreatic cancer and its significance. *Int J Clin Exp Pathol* 2015;8:6724–6731.
 39. Wei D, Wang L, Yan Y, Jia Z, Gagea M, Li Z, Zuo X, Kong X, Huang S, Xie K. KLF4 is essential for induction of cellular identity change and acinar-to-ductal reprogramming during early pancreatic carcinogenesis. *Cancer Cell* 2016;29:324–338.
 40. He P, Yang JW, Yang VW, Bialkowska AB. Kruppel-like factor 5, increased in pancreatic ductal adenocarcinoma, promotes proliferation, acinar-to-ductal metaplasia, pancreatic intraepithelial neoplasia, and tumor growth in mice. *Gastroenterology* 2018;154:1494–1508 e13.
 41. Orlandini LF, Reis F, da Silveira WA, Tiezzi MG, de Andrade JM, Silva AR, Deaton R, Bosland M, Tizzi DG. Identification of a subtype of poorly differentiated invasive ductal carcinoma of the breast based on vimentin and E-cadherin expression. *Rev Bras Ginecol Obstet* 2018;40:779–786.
 42. Zheng X, Carstens JL, Kim J, Matthew Scheible, Kaye J, Sugimoto H, Wu CC, LeBleu VS, Kalluri R. Epithelial-to-mesenchymal transition is dispensable for metastasis but induces chemoresistance in pancreatic cancer. *Nature* 2015;527:525–530.
 43. Ozaki K, Kishikawa F, Tanaka M, Sakamoto T, Tanimura S, Kohno. Histone deacetylase inhibitors enhance the chemosensitivity of tumor cells with cross-resistance to a wide range of DNA-damaging drugs. *Cancer Sci* 2008;99:376–384.
 44. Aghdassi A, Sendler M, Guenther A, Mayerle J, Behn CO, Heiecke CD, Friess H, Buchler, Evert M, Lerch MM, Weiss FU. Recruitment of histone deacetylases HDAC1 and HDAC2 by the transcriptional repressor ZEB1 downregulates E-cadherin expression in pancreatic cancer. *Gut* 2012;61:439–448.
 45. Chan E, Arlinghaus LR, Cardin DB, Goff L, Berlin JD, Parikh A, Abramson RG, Yankeelov TE, Hiebert S, Merchant N, Bhaskara S, Chakravarthy AB. Phase I trial of vorinostat added to chemoradiation with capecitabine in pancreatic cancer. *Radiother Oncol* 2016;119:312–318.
 46. Pan FC, Bankaitis ED, Boyer D, Xu X, Van de Casteele M, Magnuson MA, Heimberg H, Wright CVE. Spatiotemporal patterns of multipotentiality in Ptf1a-expressing cells during pancreas organogenesis and injury-induced facultative restoration. *Development* 2013; 140:751–764.
 47. Kopinke D, Brailsford M, Pan FC, Magnuson MA, Wright XVE, Murtaugh LC. Ongoing Notch signaling maintains phenotypic fidelity in the adult exocrine pancreas. *Dev Biol* 2012;362:57–64.

Received March 5, 2019. Accepted September 9, 2019.

Correspondence

Address correspondence to: Shin Maeda, MD, PhD Department of Gastroenterology, Graduate School of Medicine Yokohama City University, 3-9 Fukuura, Kanazawa-ku, Yokohama 236-0004, Japan. e-mail: smaeda@yokohama-cu.ac.jp; fax: (81) 45-787-2327.

Acknowledgments

The authors thank Yuki Yamashita for technical assistance. We cited the mouse image with permission from the Database Center for Life Science (Japan) (2016 DBCLS TogoTV).

Author contributions

Yoshihiro Kaneta, Takeshi Sato, Yohko Hikiba, Makoto Sugimori, Soichiro Sue, Hiroaki Kaneko, Kuniyasu Irie, Tomohiko Sasaki, and Masaaki Kondo performed the research; Wataru Shibata and Makoto Chuma designed and performed the research; and Shin Maeda designed and wrote the manuscript.

Conflicts of interest

The authors disclose no conflicts.

Funding

This work was supported by the Japan Society for the Promotion of Science KAKENHI grant JP17K09465 and the Yokohama City University Kamome project.